

Partial feedback linearising force-tracking control: implementation and testing in electrohydraulic actuation

B. Ayalew and K.W. Jablokow

Abstract: The implementation, testing and performance evaluation of a partial feedback linearising force tracking controller on an electrohydraulic actuator is described. The underlying assumptions necessary for the development of the controller are highlighted, and the control law is derived in detail. Performance comparisons are conducted against a linear state feedback with integral controller and a standard PID controller, the latter being the most common industrial solution. Results show that the nonlinear partial feedback linearising controller has improved tracking properties, as might be expected from its use of more modelling and feedback information. Multiple experiments are also conducted to investigate the robustness of the system to certain model parameters; it is shown that the controller tolerates a measurable shift in these parameters.

Nomenclature

A_b, A_t	piston areas for the bottom and top chambers, respectively	\bar{i}_v	net servovalve current
$C_{d,i}; i = 1, 2, 3, 4$	discharge coefficient	$i_{v\text{off}}$	offset current to account for abrasion wear and lap conditions
C_L	leakage coefficient used in controller	k_1	positive constant gain in closed-loop system (22)
C_{Lb}, C_{Lt}	leakage coefficients computed from (35) and (36)	k_0	constant positive gain of closed-loop system (17)
C_v	valve coefficient used in controller	$K_{v,i}; i = 1, 2, 3, 4$	valve coefficients defined by (29)
$C_{v,i}; i = 1, 2, 3, 4$	valve coefficient referred to each port	m_p	lumped mass of piston, fixture and oil mass in cylinder
e_F	pressure force tracking error	p_b, p_t	pressure in the bottom and top cylinder chambers, respectively
f_F	nonlinear feedback term given by (12)	p_L	load or differential pressure ($p_L = p_b - p_t$)
F_f	friction force on piston	p_R	return pressure at servovalve
F_L	load force or specimen reaction on piston	p_S	supply pressure at servovalve
$F_{L,d}$	desired or reference load force trajectory	q_b, q_t	flow to the bottom and from the top cylinder chambers, respectively
F_p	fluid pressure force on piston	$q_{e,b}, q_{e,t}$	external leakage from the bottom and top chambers, respectively
$F_{p,d}$	desired or reference pressure force trajectory	q_i	internal leakage in cylinder
f_{pL}	nonlinear feedback term given by (9)	u_1, u_2, u_3, u_4	underlap or overlap lengths for servovalve spool
g_F	nonlinear feedback term given by (13)	V_b, V_t	bottom and top cylinder chamber volumes, respectively
g_{pL}	nonlinear feedback term given by (10)	v_p	piston velocity
G_V	static gain of the valve	w_i	port widths
i, k	indexing integers	x	dummy variable
i_v	servovalve current	x_p	piston position
		x_v	servovalve spool displacement
		$x_{v\text{off}}$	offset spool displacement
		β_b, β_t	estimated bulk modulus for bottom and top chambers, respectively
		β_e	effective bulk modulus

© The Institution of Engineering and Technology 2007

doi:10.1049/iet-cta:20060186

Paper first received 25th April and in revised form 26th August 2006

B. Ayalew is with the Department of Mechanical Engineering, Clemson University, 227 Flour Daniel EIB, Clemson, SC, 29634

K.W. Jablokow is with Great Valley School of Graduate Professional Studies, Pennsylvania State University, 30 E. Swedesford Road, Malvern, PA 19355, USA

E-mail: beshah@clemson.edu

1 Introduction

1.1 Electrohydraulic actuation

In many industrial applications involving force generation, electrohydraulic actuators are often better choices than their rival electromechanical actuators because of their higher load stiffness, higher level of self-cooling and higher power-to-weight ratio. However, electrohydraulic actuators exhibit significant nonlinearities in their dynamics, which may necessitate the use of more elaborate control techniques than the ubiquitous PID loops.

The literature offers a wide variety of methods for improving the position and force tracking performance of electrohydraulic actuators. These include variants of linear state feedback [1], adaptive control [1–5], variable-structure control [6, 7] and Lyapunov-based controller designs [5, 8–11]. Each approach has its own strengths and limitations, which are outlined in the respective references listed above. In this work, our focus is to evaluate a partial feedback linearisation approach to force tracking control using experiments on an electrohydraulic actuator designed for a fatigue testing application.

1.2 Feedback linearisation

Feedback linearisation involves the transformation of a non-linear system to a linear one via state feedback and input transformation. A formal theory of feedback linearisation is detailed in the texts by Slotine and Li [12] and Khalil [13]; the method applies to systems whose model structure permits such transformations to be performed. As will be shown in Section 3, under some specific assumptions, the model of an electrohydraulic actuator can be formulated in a way that approaches a partial feedback linearisable or input–output (IO) linearisable form.

Perhaps the earliest study on the application of feedback linearisation to electrohydraulic actuators was that of Axelson and Kumar [14] in 1988. Their work presented the derivation of the control law, emphasising the nonlinearity for valve orifice flow only; no simulation or experimental results were published. Hahn *et al.* [15] derived a more detailed controller for the position-tracking case, including the major nonlinearities arising from valve flow and non-linear hydraulic compliance; they presented limited results from a computer simulation study only. Vossoughi and Donath [16] presented the analysis and derivation of a feedback linearising controller for velocity tracking. Del Re and Isidori [17] discussed the application of feedback linearisation to approximate models obtained by replacing the original nonlinear system model with linear–bilinear cascade model interconnections. The monograph by Jeali and Kroll [1] summarises generalised nonlinear control structures from various references, including feedback linearisation results; however, it focuses on position-control applications and presents limited experimental results.

In this paper, our goal is to describe the development, testing and performance evaluation of a partial feedback linearising pressure force controller using an electrohydraulic actuator testbed. Unlike some of our previous work [18], the derivation of the controller law in this paper uses the load pressure description only; the result is a simplified controller expression that is valid under certain relevant assumptions.

2 Electrohydraulic test system and modelling

The electrohydraulic system under consideration consists of a 5 gpm (19 lpm) two-stage servovalve close-coupled with a

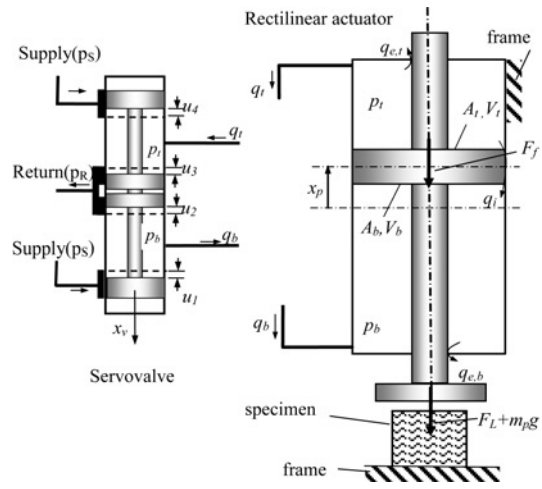


Fig. 1 Schematic of servovalve and actuator

10 kN, 102 mm-stroke symmetric actuator. The actuator is mounted on a load frame for a fatigue testing application (Fig. 1).

Fig. 1 shows a piston actuator with two hydraulic flow rates: q_t from the top chamber and q_b to the bottom chamber of the cylinder. Leakage flow between the two chambers is either internal (q_i) between the two chambers or external from the top chamber ($q_{e,t}$) and from the bottom chamber ($q_{e,b}$). A_t and A_b are the effective piston areas of the top and bottom faces, respectively. V_t and V_b are the volumes of oil in the top and bottom chambers of the cylinder, respectively, corresponding to the centre position ($x_p = 0$) of the piston. These volumes are assumed to include the respective volumes of oil in the pipelines between the servovalve and actuator, as well as the small volumes in the servovalve itself. It is assumed here that the pressure dynamics in the lines between the servovalve and the actuator are negligible owing to the close-coupling (i.e. any resonances introduced by the short-length lines are well above the frequency range of interest for the system).

Physical models of electrohydraulic servo-actuators are quite widely available in the literature [1, 8, 19–24]. The system model adopted for this work is detailed in Appendix A.

3 Control law derivation

3.1 Model reduction

For the control law derivation in this paper, the servovalve is considered to be critically centred, with symmetric and matched orifices. That is, the underlap/overlap lengths are neglected. Instead, an offset value of the valve position can be estimated during calibration to take into account any abrasion-induced null offsets [20]. Also, the valve spool dynamics are ignored. This implies that the valve spool position is assumed to be related to the servovalve current with a static gain, as given by

$$\bar{i}_v = G_v \bar{x}_v \quad (1)$$

where $\bar{i}_v = i_v - i_{v\text{off}}$ and $\bar{x}_v = x_v - x_{v\text{off}}$, with $i_{v\text{off}}$ and $x_{v\text{off}}$ representing the current offset and valve spool position offset, respectively. In this case, either the servovalve current or the valve spool position can be considered as the control variable. Since the valve spool position measurement is not available for the test system under consideration, and also to maintain consistency with the true

control input, only the servovalve current is used as the control variable in this paper.

The flow rates to and from the cylinder chambers are then rewritten as follows

$$q_b = C_{v,1} \text{sg}(\bar{i}_v) \text{sgn}(p_S - p_b) \sqrt{|p_S - p_b|} - C_{v,2} \text{sg}(-\bar{i}_v) \text{sgn}(p_b - p_R) \sqrt{|p_b - p_R|} \quad (2)$$

$$q_t = C_{v,3} \text{sg}(\bar{i}_v) \text{sgn}(p_t - p_R) \sqrt{|p_t - p_R|} - C_{v,4} \text{sg}(-\bar{i}_v) \text{sgn}(p_S - p_t) \sqrt{|p_S - p_t|} \quad (3)$$

where the new valve coefficients referenced to the current are given by

$$C_{v,i} = G_v K_{v,i}, \quad i = 1, 2, 3, 4 \quad (4)$$

The form of the flow rate (2) and (3) makes it possible to estimate the actual valve coefficients from experimental data (see Appendix B). The system model can be simplified further by introducing the so-called load pressure or differential pressure

$$p_L = p_b - p_t \quad (5)$$

When the valve ports are matched and symmetrical ($C_{v,1} = C_{v,2} = C_{v,3} = C_{v,4} = C_v$), it can be shown that [21]

$$p_b = \frac{1}{2}(p_S + p_R + p_f) \quad (6)$$

$$p_t = \frac{1}{2}(p_S + p_R + p_L) \quad (7)$$

With these expressions, the state equations for the chamber pressures can be replaced with a single state equation for the load pressure

$$\dot{P}_L = f_{p_L}(x_p, \dot{x}_p, p_L) + g_{p_L}(x_p, p_L, \text{sgn}(\bar{i}_v))\bar{i}_v \quad (8)$$

where

$$f_{p_L}(x_p, \dot{x}_p, p_L) = -\beta_e \dot{x}_p \left(\frac{A_b}{V_b + A_b x_p} + \frac{A_t}{V_t - A_t x_p} \right) - \beta_e C_L p_L \left(\frac{1}{V_b + A_b x_p} + \frac{1}{V_t - A_t x_p} \right) \quad (9)$$

$$g_{p_L}(x_p, p_L, \text{sgn}(\bar{i}_v)) = \beta_e C_v \sqrt{\left(\frac{p_S - p_R}{2} \right)} \sqrt{1 - \frac{p_L}{p_S - p_R} \text{sgn}(\bar{i}_v)} \times \left(\frac{1}{V_b + A_b x_p} + \frac{1}{V_t - A_t x_p} \right) \quad (10)$$

This reduces the order of the modelled system from four to three, the relevant state equations being (31), (32) (in Appendix A) and (8).

3.2 Pressure force tracking control

For a symmetric actuator ($A_b = A_t = A_p$), the pressure force dynamics is given by

$$\dot{F}_p = A_p \dot{p}_L = f_F(x_p, \dot{x}_p, p_L) + g_F(x_p, p_L, \text{sgn}(\bar{i}_v))\bar{i}_v \quad (11)$$

where

$$f_F(x_p, \dot{x}_p, p_L) = A_p f_{p_L}(x_p, \dot{x}_p, p_L) \quad (12)$$

$$g_F(x_p, p_L, \text{sgn}(\bar{i}_v)) = A_p g_{p_L}(x_p, p_L, \text{sgn}(\bar{i}_v)) \quad (13)$$

Equation (11), with f_F and g_F defined by (12) and (13), respectively, contains all the major modelled nonlinearities in the hydraulic system arising from fluid compliance and turbulent orifice flow. Also, the derivative of the output piston force, F_p , is seen to be only piecewise-linear in the control input (\bar{i}_v). This suggests that a partial feedback linearisation [an input–output (IO) linearisation] with a relative degree 1 can be performed in the respective domains ($\bar{i}_v > 0$ and $\bar{i}_v < 0$) [12, 13]. Furthermore, the nonlinearities in the piston force dynamics (11) can be cancelled by choosing the piecewise IO linearising control input as follows

$$\bar{i}_v = \frac{1}{g_F(x_p, p_L, \text{sgn}(\bar{i}_v))} (v - f_F(x_p, \dot{x}_p, p_L)) \quad (14)$$

where v is a new (transformed) control input. The piston force dynamics (11) reduces to

$$\dot{F}_p = v \quad (15)$$

This is a simple linear integrator, which can easily be stabilised by state feedback. Exponentially convergent tracking of a desired differentiable piston force profile ($F_{p,d}$) can be achieved by choosing v as follows

$$v = \dot{F}_{p,d} - k_0(F_p - F_{p,d}) \quad (16)$$

The force tracking error dynamics is given by

$$\dot{e}_F + k_0 e_F = 0 \quad (17)$$

where e_F is the force tracking error, $e_F = F_p - F_{p,d}$.

In summary, the control input of (14), with v given by (16) and a proper choice of $k_0 > 0$, can give a desired degree of exponential force tracking performance, regardless of the nonlinearities in (8), provided the internal dynamics are stable. In terms of the force tracking error, the control current is given by

$$\bar{i}_v = \frac{1}{g_F(x_p, p_L, \text{sgn}(\bar{i}_v))} (\dot{F}_{p,d} - k_0 e_F - f_F(x_p, \dot{x}_p, p_L)) \quad (18)$$

It is important to note that (18) cannot be solved ‘as is’, since it contains the control variable, \bar{i}_v , on both sides of an equation involving the sgn function. A practical solution to this problem becomes evident when considering the digital implementation of the piecewise IO linearising controller. The sign of the value of \bar{i}_v at the previous time step can be used to compute the value of \bar{i}_v at the current time step, if it can be supposed that the current does not change sign at a rate faster than the sampling rate. In fact, the sampling rate for the digital implementation could be so chosen to impose such conditions. However, it is difficult to prove analytically that this approach does not lead to control chatter. This chatter problem has not previously been reported in the literature that discusses feedback linearisation for hydraulic drives [15–18]. In addition, the problem has not been experienced during any of the position- and force-control experiments conducted by the authors under this assumption [25, 26].

The name ‘near-input–output (near-IO) linearisation’ is adopted in this paper to make the explicit distinction that the present controller is not a true partial feedback (or input-output) linearising controller in the traditional sense,

but it is very close. The piecewise IO linearisation gave a system of relative degree 1 in each domain. That is, only one differentiation of the output was needed before the input appeared. The external dynamics is given by (15). It remains to evaluate the stability of the internal dynamics of degree 2, involving system states that are rendered ‘unobservable’ during the piecewise IO linearisation. It can be shown that the internal dynamics can be described using the piston position and velocity as the internal state variables, from which the internal stability is readily established using (31) and (32) (Appendix A) [13].

It is worth mentioning at this point that had the valve dynamics been included in the system model, the sgn function would be acting on the valve spool position (x_v , see (26) and (27) in Appendix A), that is, on a state variable instead of a control input (i_v). This would remove the need to make the explicit assumption for the near-IO linearisation discussed above, at the cost of requiring further model knowledge about the servovalve. Others have studied such cases [27, 28]. Our focus here is to document some experimental results for the near-IO linearising controller (18) as described above.

A schematic of the implementation of the near-IO linearising controller (NLC) is shown in Fig. 2. It should also be noted that the pressure force-control problem and the differential or load pressure-control problem differ only by a factor of the piston area (for a symmetric actuator). Therefore, the force control conclusions discussed in this paper apply equally well to the differential pressure-control case.

3.3 Load force tracking control

This subsection is included to highlight aspects of the near-IO linearisation approach to the control of the net force applied to the specimen, that is, control of the load force (F_L). This force is given by

$$F_L = F_p - F_f - m_p(g + \ddot{x}_p) \quad (19)$$

Differentiating (19) and using (11), we obtain

$$\begin{aligned} \dot{F}_L = & f_F(x_f, \dot{x}_p, p_L) - \dot{F}_f - m_p(\ddot{x}_p) \\ & + g_F(x_p, p_L, \text{sgn}(\tilde{i}_v))\tilde{i}_v \end{aligned} \quad (20)$$

Proceeding as described in Section 3.2, the near-IO linearising controller with this definition of system output can be

shown to be

$$\begin{aligned} \tilde{i}_v = & \frac{1}{g_F(x_p, p_L, \text{sgn}(\tilde{i}_v))} (\dot{F}_{L,d} - k_1(F_L - F_{L,d}) \\ & - f_F(x_p, \dot{x}_p, p_L) - \dot{F}_f - m_p(\ddot{x}_p)) \end{aligned} \quad (21)$$

Here, the gain k_1 is chosen to stabilise the closed-loop force tracking error dynamics, as follows

$$(\dot{F}_L - \dot{F}_{L,d}) + k_1(F_L - F_{L,d}) = 0 \quad (22)$$

It can be seen that the load force-tracking controller given by (21) needs additional variables for feedback, as compared with that given in (18): namely, the derivatives of the friction force, the inertia force and the load force. It is particularly important that an accurate and differentiable approximation of the friction force be found. While these problems can be approximated in various ways, they are not pursued in this paper.

4 Experiments

The experiments in this section consider a realistic loading on a fatigue test specimen. The tacit assumptions of no piston motion and hence limitation of the test force magnitudes to below static friction values, will not be necessary [8, 29]. The piston is constrained instead with a neoprene rubber specimen so that large force magnitudes can be absorbed. In the experiments presented here, the force magnitudes were selected such that the specimen was always in compression (for convenience with specimen mounting), but there should be no loss of generality for the observations.

Since the NLC uses the derivative of the reference (desired) force trajectory, smooth desired force trajectories need to be used. In particular, to compare step responses, the Heaviside step function (which has sharp corners) was approximated by a differentiable function involving the hyperbolic tangent function. The experimental system uses an LVDT for position measurement, which is low-pass filtered with a cut-off frequency of 30 Hz before differentiating the signal to obtain the piston velocity. The differential pressure feedback from two chamber pressure transducers was used to compute the pressure force. The sampling rate was set at 1 kHz.

4.1 Nominal performance comparison

The nominal NLC is the nonlinear controller given by (18), employing the nominal model parameters for the effective bulk modulus β_e , the valve coefficient C_v , the leakage

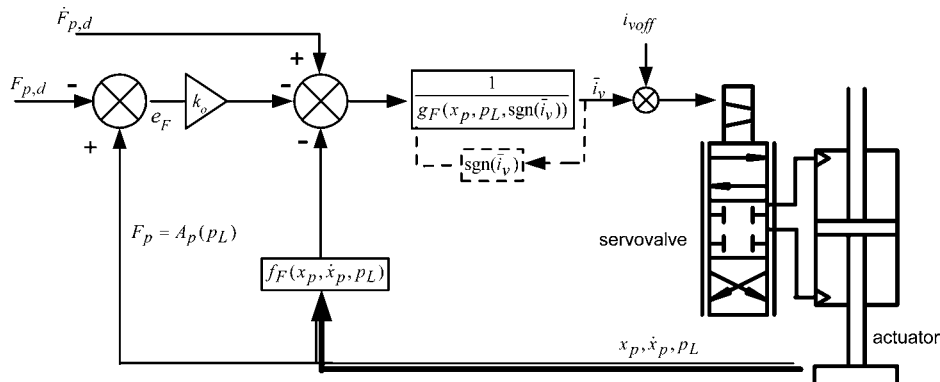


Fig. 2 Schematic of the implementation for the near-IO linearising controller

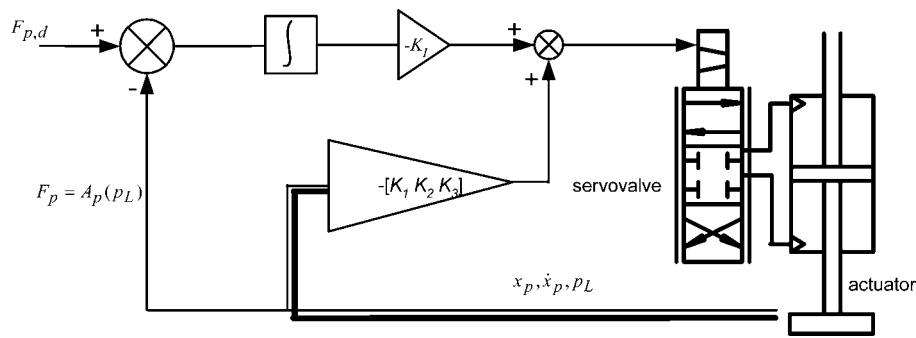


Fig. 3 Schematic of implementation for the linear state feedback with integral controller

coefficient C_L , and the supply (p_S) and return (p_R) pressures at the servovalve. The first three model parameters can be estimated using simple experiments (Appendix A). The last two are known to change dynamically with the dynamics of supply and return hoses and accumulators. Here, we consider limited-bandwidth experiments such that the frequency ranges of interest are below the influence of these line dynamics.

For a comparison of the performance of the NLC with standard linear controllers, a PID controller and a controller employing linear state feedback with integral (LSFI) control are considered. The latter uses feedback of the same states as the NLC, as can be seen by comparing the schematics given in Figs. 2 and 3. The PID gains were tuned by starting with a Ziegler–Nichols [30] estimate applied to a locally linearised model and fine-tuning the experimental implementation. The final gains taken were those that gave least steady-state error, with the least overshoot and shortest rise time and settling time.

To design the LSFI controller, a local linearisation (Jacobian linearisation) of the reduced nonlinear model of Section 3.1 was used. Various closed-loop pole-location combinations were attempted, including optimal recommendations from performance criteria, such as the integral of time multiplied by the absolute error (ITAE) criterion [24] and locations based on standard Bessel filters. The gains computed from these pole locations

resulted in a very oscillatory response when implemented on the experimental system for closed-loop bandwidth choices as small as 10 Hz. The final approach adopted here was to start with the open-loop pole locations of the linear model and shift only the poles located close to the $-j\omega$ axis until the LSFI controller using the corresponding gains gave a good, oscillation-free level of tracking.

Fig. 4 shows a basic comparison of the NLC with a gain setting of $k_0 = 750 \text{ s}^{-1}$, the well-tuned PID controller, and the LSFI controller. It can be seen from Fig. 4 that owing to the overshoot in the force response with the PID controller, the specimen was compressed the most (piston travel was the highest) and the magnitude of the control current required was the highest in the PID control case. The LSFI controller resulted in a sluggish force response with the least piston travel. The performance of the NLC was the best of the three, considering the rise time and settling time, the absence of overshoot in the force response, as well as the magnitude of the control current.

Further comparison can be made between these controllers by looking at the sinusoidal force-tracking responses shown in Fig. 5, with the same gain settings as above. At higher frequencies, the force output associated with the NLC starts to show increased phase lag, as do the linear controllers. However, the reduction in output force magnitude associated with the NLC is not as great as it is with the linear controllers. In certain applications, such as with the

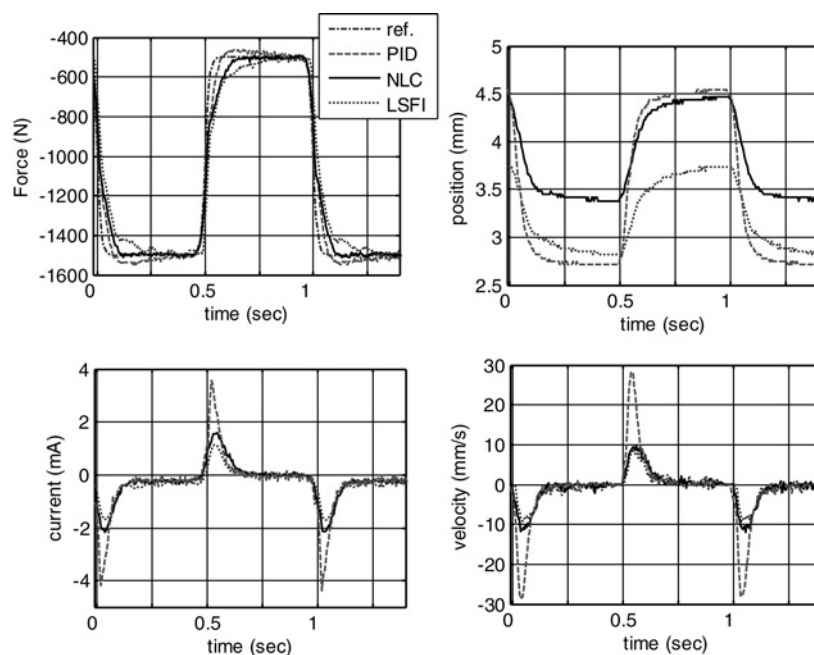


Fig. 4 Experimental comparison of the nominal tracking performance

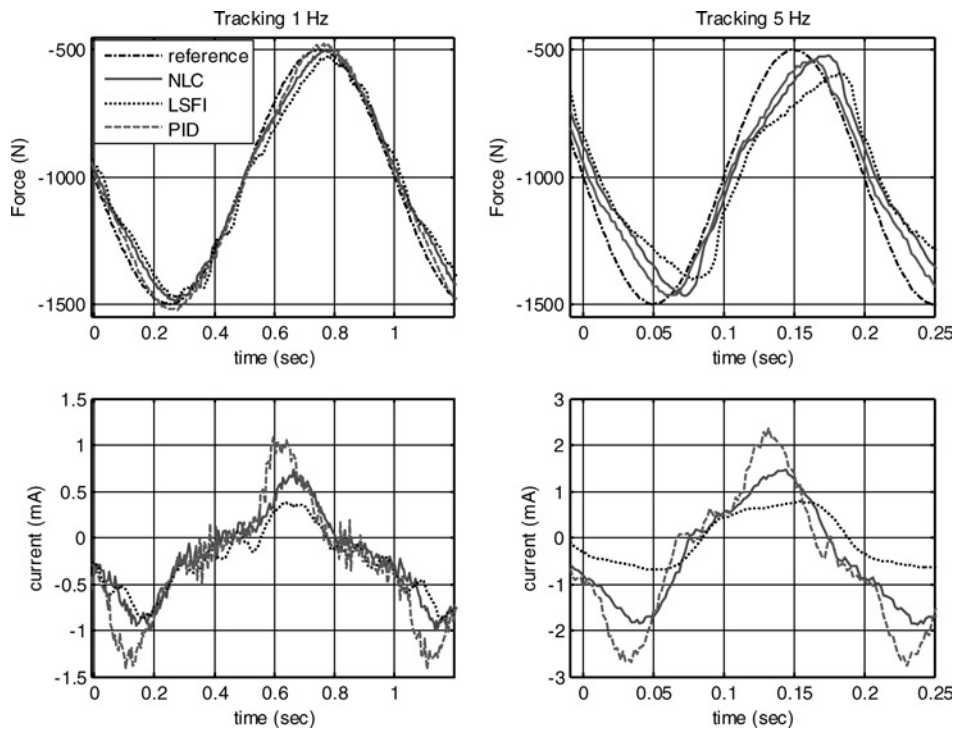


Fig. 5 Experimental comparison tracking sinusoidal force trajectories

fatigue testing of certain specimens, it may be necessary to reduce force magnitude errors and tolerate phase lags, in which case the NLC has a clear advantage. Also, it should be noted that the NLC uses consistently lower current peak magnitudes (of the order of 40% lower than the PID controller). However, it should be expected that the performance of the NLC will eventually deteriorate at higher frequencies (as does that of the linear controllers) owing to effects from neglected supply- and return-line dynamics, as well as the neglected servovalve dynamics during controller derivations.

Two reasons can be given for the observed superiority of the NLC. First, recall that with the cancellation of the first term in the function f_F (see (9) and (18)), the dynamics of the piston motion is decoupled from the pressure force dynamics. This allowed us to push the possible closed-loop pole location ($s = -k_0$) of the pressure force dynamics much farther to the left in the s -plane than was possible with the two linear controllers without exciting oscillations. A second reason for the observed superiority of the NLC is the nonlinearity cancellation, as explicitly included in both the f_F and g_F terms of the NLC (18).

The NLC can be tuned by the single parameter k_0 , for a range of settling times and rise times, as shown in Fig. 6. As the gain k_0 was increased, the rise time decreased, with a corresponding increase in the control current. Above a certain magnitude of the gain ($k_0 = 1500 \text{ s}^{-1}$), the force response exhibited overshoot and started to include undesirable oscillations. Lower values of the gain gave sluggish responses.

Steady-state errors were observed to be functions of the null offset (i_{voff}), which amounted to internal cross-port leakage in the valve. For these experiments, the latter was reduced as much as possible by careful use of the mechanical null adjustment on the servovalve.

4.2 Robustness to model parameters

A common concern regarding the use of model-based feedback linearising controllers is that they could be sensitive to

model-parameter variations. For the system under consideration, the relevant model parameters that appear in the controller expression are the effective bulk modulus β_e , the valve coefficient C_v , the leakage coefficient C_L , and the supply (p_S) and return (p_R) pressures at the servovalve. The effects of the latter two parameters enter into the system dynamically owing to the rather long transmission hoses used with the present test system. In this section, experimental results are presented outlining the sensitivity of the performance of the NLC to changes in β_e , C_v , and C_L . One of the parameters is changed, while nominal values are kept for the other parameters in the NLC expression.

Fig. 7 shows the effect of uncertainty in the effective bulk modulus β_e . The experiments were conducted by changing β_e by a factor of more than $\pm 50\%$ of the nominal value of 850 MPa. The lower the value of β_e used in the controller, the shorter the rise time, and the higher the tendency to overshoot and exhibit oscillations in the force response. On the other hand, the higher the value of β_e used in the

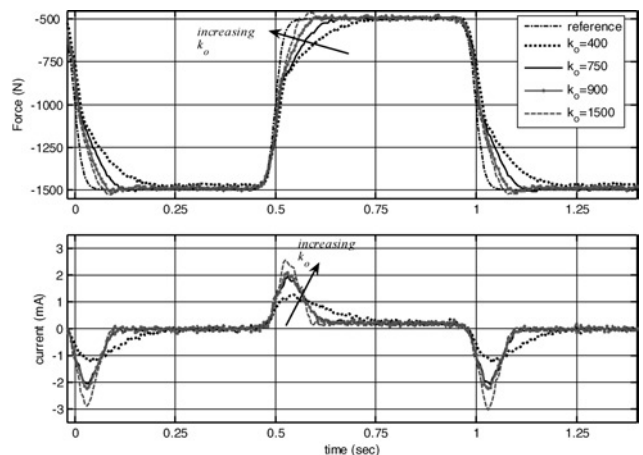


Fig. 6 Near-IO linearising controller tuned with gain k_0

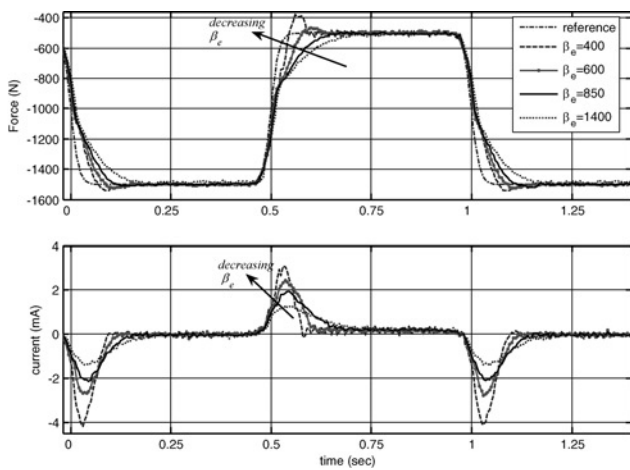


Fig. 7 Robustness to changes in the bulk modulus parameter of the near-IO linearising controller

controller, the more sluggish the response became. This also implies that if there were a reduction in the actual value of the effective or working bulk modulus of the oil in the system (from what was set in the controller expression), the controller performance improves or deteriorates in the manner depicted in Fig. 7. In practice, changes in the effective bulk modulus of the fluid in a hydraulic system could happen for various reasons, such as air entrapment (aeration), changes in mechanical compliance and changes in temperature.

It was also observed that the system was more sensitive to decreasing changes in β_e than to increasing changes. The response started to overshoot with only a 25% reduction of the value of β_e , while the response remained virtually the same as the nominal case for a 25% increase in the value of β_e . The faster responses, corresponding to lower β_e settings, also required higher current peak magnitudes, as shown in the lower plot of Fig. 7. For example, for a 25% reduction in the value of β_e , the current peak required was as much as 100% higher than the current peak with nominal settings for β_e .

Fig. 8 shows the effect of uncertainty in the estimation of the valve coefficient parameter C_v . The experiments were conducted by changing C_v by a factor of approximately $\pm 25\%$ of the nominal value of $2.75 \text{ cm}^3 \text{ s}^{-1} \text{ mA}^{-1} \text{ MPa}^{-1/2}$, while keeping the other parameters at their respective nominal values. The observed trend is similar to the effect of changes in β_e . Here, however, the response started to show overshoot

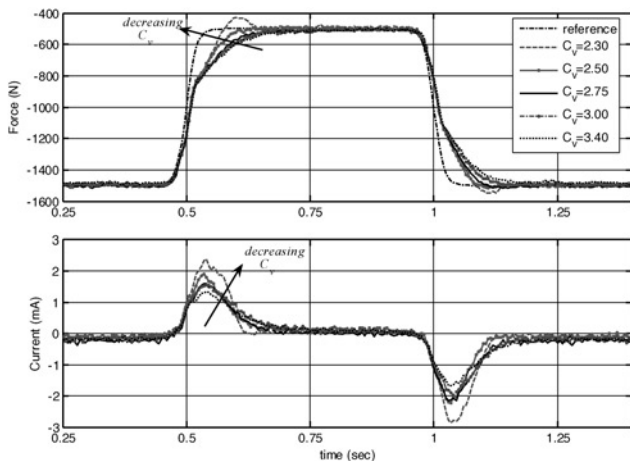


Fig. 8 Robustness to changes in the valve coefficient parameter of the near-IO linearising controller

with only a 16% reduction in the value of C_v , whereas it remained less sensitive to increasing the value of C_v by as much as 25% of the nominal value. These observations imply that in the controller implementation, it is better to overestimate C_v and β_e in order to avoid overshoot and oscillations in the force response.

There remains some asymmetry in the force responses and control current inputs for the application and removal of the step-force reference with the up and down motions of the piston. These can be explained by the fact that a single value of the valve coefficient was used in the experiments for all valve ports, despite the identification data indicating a slight asymmetry. Furthermore, the motion of the piston is influenced by the nonlinear compliance of the neoprene rubber, which is known to exhibit hysteretic behaviour.

Finally, Fig. 9 shows the effect of the leakage coefficient C_L on the performance of the NLC. In these experiments, C_L changed by as much as 200% of the nominal value of $0.5 \text{ cm}^3 \text{ s}^{-1} \text{ MPa}^{-1}$. This range is exaggerated, including a hypothetical negative leakage coefficient, to magnify the observed response.

The effect of the leakage coefficient appears to be causing offset and steady-state error. The control current does not appear to be affected significantly by changes in the settings for the leakage coefficient C_L , and so is not shown here. The asymmetry in the response is attributed once again to the averaging adopted for the valve and leakage coefficients and the hysteretic behaviour of the specimen.

5 Summary and conclusions

One goal of this paper was to document the experimental validation and testing of the near-IO linearising controller (NLC). This nonlinear force tracking controller was developed based on partial feedback linearisation (precisely, a near-input-output linearisation) of a nonlinear model of an electrohydraulic actuator. This linearisation allows cancellation of the nonlinearity introduced by valve orifice flow and position-dependent compliance. Supply- and return-line effects and the servovalve dynamics were neglected for deriving the controller, but the controller was implemented on a realistic system subjected to these effects.

Experimental comparisons with standard linear controllers for tracking reference pressure force signals showed

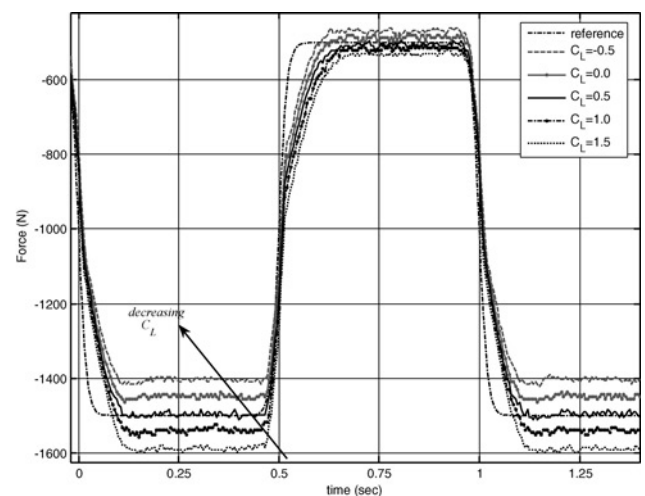


Fig. 9 Robustness to changes in the leakage coefficient parameter of the near-IO linearising controller

that the NLC with nominal model parameters gave a compromise tracking performance between a well-tuned PID controller (for which some overshoot had to be accepted for zero steady-state error) and a sluggish linear state feedback with integral controller designed using pole placement techniques on a locally linearised model of the system. Even though we cannot claim that this comparison was exhaustive for all such systems and loading conditions, it appears that the NLC for pressure force-tracking performs better than a PID controller for properly selected gain settings. This should be expected, as the NLC uses more information (in feedback and/or nonlinearity cancellation) than either the PID or linear state-feedback controllers. It was also shown that the NLC presented in this paper can be tuned by using the single linear gain (k_0) within limits, depending on the acceptable level of overshoot and the desired speed of response.

The robustness of the model-based NLC to model parameters was also studied. It was observed that the response slowed down only slightly for as much as 25% higher than nominal settings of the effective bulk modulus and valve coefficient parameters. However, the response started to show overshoot and oscillation for lower than nominal settings of about 16% for C_v and 25% for β_e . Nevertheless, the experiments suggest that the NLC tolerates a measurable shift in the values of these parameters. This result is particularly interesting for the effective bulk modulus parameter, whose value is generally difficult to predict in a hydraulic system. Finally, the effect of changing the leakage coefficient setting in the NLC was seen to produce a steady-state error.

Further work with the NLC pressure force tracking presented in this paper will involve extensions to a formal robust controller such as sliding-mode and/or adaptive controllers that take into account the parameter bounds identified above. In addition, the nonlinearity cancellation, and thereby the reduction of the pressure force dynamics to a linear force error dynamics, by the NLC, allows one to view the electrohydraulic actuator as a linear force generator. The latter interpretation can be used to design independently tuneable position controllers by synthesising a desired force trajectory for the force generator, as is shown in [31].

6 Acknowledgments

The authors would like to thank the late Professor Bohdan T. Kulakowski of Pennsylvania State University who was closely involved with this work and supported it to completion.

The experiments in this work were conducted at the Pennsylvania Transportation Institute of Pennsylvania State University, University Park, PA 16802, USA.

7 References

- 1 Jelali, M., and Kroll, A.: 'Hydraulic servo-systems: modelling, identification and control' (Springer-Verlag, London, 2003)
- 2 Plummer, A.R., and Vaughan, N.D.: 'Robust adaptive control for hydraulic servosystems', *Trans. ASME, J. Dyn. Syst. Meas. Control*, 1996, **118**, pp. 237–244
- 3 Yun, J.S., and Cho, H.S.: 'Application of an adaptive model following control technique to hydraulic servo system subjected to unknown disturbances', *Trans. ASME, J. Dyn. Syst. Meas. Control*, 1991, **113**, pp. 470–486
- 4 Ziaei, K., and Sepheri, N.: 'Design of a nonlinear adaptive controller for an electrohydraulic actuator', *J. Dyn. Syst. Meas. Control*, 2001, **123**, pp. 449–456

- 5 Alleyne, A., and Hedrick, K.J.: 'Nonlinear adaptive control of active suspensions', *IEEE Trans. Control Syst. Tech.*, 1995, **3**, (1), pp. 94–101
- 6 Liu, Y., and Handroos, H.: 'Applications of sliding mode control to an electrohydraulic servosystem with flexible mechanical load'. Proc. 4th Int. Conf. on Motion and Vibration Control (MOVIC), Zurich, Switzerland, 25–28 August 1998
- 7 Nguyen, Q.H., Ha, Q.P., Rye, D.C., and Durrant-Whyte, H.F.: 'Force/position tracking for electrohydraulic systems of a robotic excavator'. Proc. 39th IEEE Conf. on Decision and Control, Sydney, Australia, December 2000
- 8 Sohl, G.A., and Bobrow, J.E.: 'Experiments and simulations on the nonlinear control of a hydraulic servosystem', *IEEE Trans. Control Syst. Tech.*, 1999, **7**, (2), pp. 238–257
- 9 Sun, H., and Chiu, G.T.-C.: 'Motion synchronization for multi-cylinder electro-hydraulic system'. Proc. 2001 IEEE/ASME Int. Conf. on Advanced Intelligent Mechatronics, Como, Italy, 8–12 July 2001, pp. 636–641
- 10 Sirouspour, M.R., and Salcudean, S.E.: 'On the nonlinear control of hydraulic servosystems'. Proc. IEEE Int. Conf. on Robotics and Automation, San Francisco, CA, April 2000, pp. 1276–1282
- 11 Hwang, C.-L.: 'Sliding mode control using time-varying switching gain and boundary layer for electrohydraulic position and differential pressure control', *IEE Proc., Control Theory Appl.*, 1996, **143**, (4), pp. 325–332
- 12 Slotine, J.-J.E., and Li, W.: 'Applied nonlinear control' (Prentice-Hall, Englewood Cliffs, NJ, 1991)
- 13 Khalil, H.K.: 'Nonlinear systems' (Prentice-Hall, Upper Saddle River, NJ, 2002, 3rd edn.)
- 14 Axelson, S., and Kumar, K.S.P.: 'Dynamic feedback linearization of a hydraulic valve-actuator combination'. Proc. 1988 American Control Conf., Atlanta, GA, 15–17 June 1988
- 15 Hahn, H., Piepenbrink, A., and Leimbach, K.-D.: 'Input/output linearization control of an electro servo-hydraulic actuator'. Proc. 3rd IEEE Conf. on Control Applications, Glasgow, UK, 1994, pp. 995–1000
- 16 Vossoughi, G., and Donath, M.: 'Dynamic feedback linearization for electrohydraulically actuated control systems', *Trans. ASME, J. Dyn. Syst. Meas. Control*, 1995, **117**, pp. 468–477
- 17 Del Re, L., and Isidori, A.: 'Performance enhancement of nonlinear drives by feedback linearization of linear-bilinear cascade models', *IEEE Trans. Control Syst. Tech.*, 1995, **3**, (3), pp. 299–308
- 18 Ayalew, B., Kulakowski, B.T., and Jablowski, K.W.: 'A near input-output linearizing force tracking controller for an electrohydraulic actuator'. Proc. IMECE 2005: International Mechanical Engineering Congress and Exposition, 5–10 November 2005, Orlando, FL (ASME, 2005)
- 19 Dransfield, P.: 'Hydraulic control systems: design and analysis of their dynamics' (Springer-Verlag, London, 1981)
- 20 Kugi, A.: 'Non-linear control based on physical models' (Springer-Verlag, London, 2001)
- 21 Merritt, H.E.: 'Hydraulic control systems' (Wiley, New York, 1967)
- 22 Van Schothorst, G.: 'Modelling of long-stroke hydraulic servo-systems for flight simulator motion control and system design', PhD dissertation, Delft University of Technology, 1997
- 23 Viersma, T.J.: 'Analysis, synthesis and design of hydraulic servosystems and pipelines' (Elsevier, Amsterdam, 1980)
- 24 Watton, J.: 'Fluid power systems: modelling, simulation and microcomputer control' (Prentice-Hall, Englewood Cliffs, NJ, 1989)
- 25 Ayalew, B.: 'Nonlinear control of multi-actuator electrohydraulic systems based on feedback linearization with application to road simulation', PhD dissertation, Pennsylvania State University, 2005
- 26 Ayalew, B., and Kulakowski, B.T.: 'Nonlinear decentralized control of electrohydraulic actuators in road simulation'. Proc. IMECE 2005: International Mechanical Engineering Congress and Exposition, 5–10 November 2005, Orlando, FL (ASME, 2005)
- 27 Alleyne, A., and Liu, R.: 'A simplified approach to force control for electrohydraulic systems', *Control Eng. Pract.*, 2000, **8**, pp. 1347–1356
- 28 Liu, R., and Alleyne, A.: 'Nonlinear force/pressure tracking of an electro-hydraulic actuator', *Trans. ASME, J. Dyn. Syst. Meas. Control*, 2000, **122**, pp. 232–237
- 29 Tafazoli, S., de Silva, C.W., and Lawrence, P.D.: 'Tracking control of an electrohydraulic manipulator in the presence of friction', *IEEE Trans. Control Syst. Tech.*, 1998, **6**, (3), pp. 401–411
- 30 Franklin, G.F., Powell, J., and Emami-Naeini, A.: 'Feedback control of dynamic systems' (Prentice-Hall, Upper Saddle River, NJ, 2006, 5th edn.)
- 31 Ayalew, B., and Kulakowski, B.T.: 'Cascade tuning for nonlinear position control of an electrohydraulic actuator'. Proc. American Control Conf., Minneapolis, MN, 14–16 June 2006

8 Appendix A: electrohydraulic system model

It can be shown that the chamber pressure dynamics are given by (see e.g. [20])

$$\frac{dp_b}{dt} = \frac{\beta_e}{V_b + A_b x_p} (q_b - A_b \dot{x}_p + q_i - q_{e,b}) \quad (23)$$

$$\frac{dp_t}{dt} = \frac{\beta_e}{V_t - A_t x_p} (-q_t + A_t \dot{x}_p - q_i - q_{e,t}) \quad (24)$$

The leakage flows $q_{e,b}$ and $q_{e,t}$ are considered negligible. The internal leakage past the piston seals is assumed here to be laminar, with a leakage coefficient C_L , as follows

$$q_i = C_L(p_t - p_b) \quad (25)$$

The predominantly turbulent flows through the sharp-edged control orifices of a spool valve to and from the two sides of the cylinder chambers are modelled by [1, 20, 21]

$$q_b = K_{v,1} \text{sg}(x_v + u_1) \text{sg}(p_S - p_b) \sqrt{|p_S - p_b|} - K_{v,2} \text{sg}(-x_v + u_2) \times \text{sg}(p_b - p_R) \sqrt{|p_b - p_R|} \quad (26)$$

$$q_t = K_{v,3} \text{sg}(x_v + u_3) \text{sg}(p_t - p_R) \sqrt{|p_t - p_R|} - K_{v,4} \text{sg}(-x_v + u_4) \text{sg}(p_S - p_t) \sqrt{|p_S - p_t|} \quad (27)$$

where the function $\text{sg}(x)$ is defined by

$$\text{sg}(x) = \begin{cases} x, & x \geq 0 \\ 0, & x < 0 \end{cases} \quad (28)$$

The parameters u_1, u_2, u_3 and u_4 are included to account for valve spool lap conditions, as shown in Fig. 1. Negative values represent overlap, while positive values represent underlap. The valve coefficients $K_{v,i}$ are given by

$$K_{v,i} = c_{d,i} w_i \sqrt{\frac{2}{\rho}}, \quad i = 1, 2, 3, 4 \quad (29)$$

These coefficients could be computed from data for the discharge coefficients $c_{d,i}$, port widths w_i and oil density ρ . Since the discharge coefficients change with service life, the ‘valve coefficients’ can and should be estimated from simple experiments, as outlined in Appendix B.

The upward force on the actuator piston due to the oil pressure is given by

$$F_p = A_b p_b - A_t p_t \quad (30)$$

The frictional force on the piston in the cylinder is denoted by F_f , and the external loadings, including specimen stiffness and damping forces, are lumped together in F_L (tensile positive). The equations of motion are derived by applying Newton’s second law, as follows

$$\dot{x}_p = v_p \quad (31)$$

$$\dot{v}_p = \frac{1}{m_p} (F_p - F_L - F_f - m_p g) \quad (32)$$

Equations (23), (24), (31) and (32), with q_b and q_t given by (26) and (27), constitute the state-space model for the servo-valve and loaded actuator subsystem under consideration. These equations also contain the major nonlinearities in the system, which are the nonlinear hydraulic compliance and the square-root flow-rate versus pressure-drop relations.

Nonlinearity is also introduced in (32) by a nonlinear frictional force and a possibly nonlinear specimen reaction F_L .

9 Appendix B: basic model and controller parameters

For the non-geometric controller parameters β_e, C_v and C_L , an offline ‘grey-box’ identification technique was adopted [1, 8]. The lap parameters u_1, u_2, u_3 and u_4 are neglected. The state (23) and (24) are discretised as follows at sampling instant k

$$\frac{V_b + A_b x_p(k)}{\beta_b} \left(\frac{dp_b}{dt}(k) \right) = q_b(k) + q_i(k) - A_b x_p(k) \quad (33)$$

$$\frac{V_t + A_t x_p(k)}{\beta_t} \left(\frac{dp_t}{dt}(k) \right) = -q_t(k) - q_i(k) + A_t x_p(k) \quad (34)$$

Discretising the flow rate (25)–(27) in the same way and regrouping variables, the following matrix form can be written

$$\begin{bmatrix} -\{V_b + A_b x_p(k)\} \left(\frac{dp_b}{dt}(k) \right) \\ D_1(k) \\ D_2(k) \\ \{p_t(k) - p_b(k)\} \end{bmatrix} \times \begin{bmatrix} \beta_b^{-1} \\ C_{v,1} \\ C_{v,2} \\ C_{Lb} \end{bmatrix} = A_b \frac{dx_p}{dt}(k) \quad (35)$$

$$\begin{bmatrix} (V_t + A_t x_p(k)) \left(\frac{dp_t}{dt}(k) \right) \\ D_3(k) \\ D_4(k) \\ (p_t(k) - p_b(k)) \end{bmatrix} \times \begin{bmatrix} \beta_t^{-1} \\ C_{v,3} \\ C_{v,4} \\ C_{Lt} \end{bmatrix} = A_t \frac{dx_p}{dt}(k) \quad (36)$$

where

$$D_1(k) = \text{sg}(i_v(k)) \text{sg}(p_S - p_b(k)) \sqrt{|p_S - p_b(k)|} \quad (37)$$

$$D_2(k) = \text{sg}(-i_v(k)) \text{sg}(p_b(k) - p_R) \sqrt{|p_b(k) - p_R|} \quad (38)$$

$$D_3(k) = \text{sg}(i_v(k)) \text{sg}(p_t(k) - p_R) \sqrt{|p_t(k) - p_R|} \quad (39)$$

$$D_4(k) = \text{sg}(-i_v(k)) \text{sg}(p_S - p_t(k)) \sqrt{|p_S - p_t(k)|} \quad (40)$$

For a given length N of the sampled data ($N > 4$), each system of (35) and (36), is linear in the unknown parameters

Table 1: Nominal values of controller parameters

Parameter	Value
β_e	850 MPa
C_v	$2.75 \text{ cm}^3 \text{ s}^{-1} \text{ mA}^{-1} \text{ MPa}^{-1/2}$
C_L	$0.5 \text{ cm}^3 \text{ s}^{-1} \text{ mA}^{-1} \text{ MPa}^{-1}$
A_p	5.08 cm^2
V_b	40.48 cm^3
V_t	34.42 cm^3
m_p	5.7 kg
p_S	13.85 MPa
p_R	0.101 MPa

of bulk modulus, valve coefficients and the leakage coefficient. Each of these systems has more equations than unknowns and is therefore solved in the least-squares sense. Estimates from several closed-loop position sine sweeps were averaged together. Furthermore, the disparate estimates of the fluid bulk modulus for the top and bottom chambers (β_t and β_b), which take on close values anyway,

were averaged together to use a single value for the effective bulk modulus, thereby simplifying the controller expression. The same was done for the valve coefficient and the leakage coefficient. These estimates of the parameters, which are listed in [Table 1](#) together with specifications of the actuator, were used as the nominal values for the control experiments.